Numerical simulation of separated flow in nozzle with slots

I.E. Ivanov[1], **I.A. Kryukov**[2], **and V.V. Semenov**[1]

[1] *Moscow Aviation Institute, Volokolamskoe shosse 4, Moscow, 125993, Russia*
[2] *Institute for Problems in Mechanics, Russian Academy of Sciences, Vernadskii avenue 101-1, Moscow, 119526, Russia*

Summary. A mathematical model and a high-resolution numerical method for numerical simulation of turbulent separated flow in convergent–divergent nozzles are presented. A comparison between numerical calculations and experimental data for plane and axi-symmetric nozzles shows an efficiency and a reasonable accuracy of a numerical code based on the proposed model. A detailed computational study of separated nozzle flows has been conducted for nozzles with one or two circular slots. The possibility for increasing in thrust efficiency is shown under ground conditions due to decreasing of overexpanded flow zone.

1 Introduction

Increase of efficiency of rocket engines due to gas dynamic control of altitude characteristics of a nozzle is considered in this paper.

Improving the power of rocket nozzles is very important to increase the payload of launchers. One of the solutions of this problem which has been obtained consists of increasing the ratio of nozzle areas and controlling the separation flow, in the overexpanded regime, during the first phase of flight. Separation moves the jet detachment point upstream, causing a change in the effective nozzle geometry to one that is shorter and has a lower expansion ratio. For a given nozzle pressure ratio, this alleviates overexpansion and improves thrust efficiency.

Several flow control technologies which have been recently proposed offers further means by which to control and stabilize a separated nozzle flow for performance enhancement. In this paper the control technology by means of creation of one or two circular slots at supersonic part of a nozzle (nozzle with slot) is considered by numerical simulation.

2 Governing Equations

The two-dimensional Favre averaged Navier-Stokes equations, including the equations for the turbulent kinetic energy (TKE) k and the solenoidal dissipation rate ε_s, can be written in the following form

$$\frac{\partial(r\mathbf{Q})}{\partial t} + \frac{\partial(r\mathbf{F})}{\partial x} + \frac{\partial(r\mathbf{G})}{\partial y} = \frac{\partial(r\mathbf{F}_v)}{\partial x} + \frac{\partial(r\mathbf{G}_v)}{\partial y} + r\mathbf{H},$$

where $\mathbf{Q} = (\overline{\rho}, \overline{\rho}\,\widetilde{u}, \overline{\rho}\,\widetilde{v}, \overline{e}, \overline{\rho}\,k, \overline{\rho}\,\varepsilon_s)^T$. The overbar denotes the conventional Reynolds average, while the overtilde is used to denote the Favre mass average. The inviscid fluxes are

$$\mathbf{F} = \begin{pmatrix} \overline{\rho}\,\widetilde{u} \\ \overline{\rho}\,\widetilde{u}^2 + \overline{p} \\ \overline{\rho}\,\widetilde{u}\,\widetilde{v} \\ \widetilde{u}(\overline{e} + \overline{p}) \\ \overline{\rho}\,\widetilde{u}\,k \\ \overline{\rho}\,\widetilde{u}\,\varepsilon_s \end{pmatrix}, \quad \mathbf{G} = \begin{pmatrix} \overline{\rho}\,\widetilde{v} \\ \overline{\rho}\,\widetilde{u}\,\widetilde{v} \\ \overline{\rho}\,\widetilde{v}^2 + \overline{p} \\ \widetilde{v}(\overline{e} + \overline{p}) \\ \overline{\rho}\,\widetilde{v}\,k \\ \overline{\rho}\,\widetilde{v}\,\varepsilon_s \end{pmatrix}.$$

where ρ is the density, u and v are the velocity components, and e is the total energy per unit volume. The fluid pressure is p and the equation of state for the perfect gas is given by

$$\overline{e} = \overline{p} + \frac{1}{2}\,\overline{\rho}\,\widetilde{u}_j\,\widetilde{u}_j + \overline{\rho}\,k,$$

where γ, the specific heat ratio, is taken as 1.4. The viscous fluxes are

$$\mathbf{F}_v = \begin{pmatrix} 0 \\ \sigma_{xx} \\ \sigma_{xy} \\ \widetilde{u}\,\sigma_{xx} + \widetilde{v}\,\sigma_{xy} - q_x \\ \left(\mu + \frac{\mu_t}{\sigma_k}\right)\frac{\partial k}{\partial x} \\ \left(\mu + \frac{\mu_t}{\sigma_\varepsilon}\right)\frac{\partial \varepsilon_s}{\partial x} \end{pmatrix}, \quad \mathbf{G}_v = \begin{pmatrix} 0 \\ \sigma_{xy} \\ \sigma_{yy} \\ \widetilde{u}\,\sigma_{xy} + \widetilde{v}\,\sigma_{yy} - q_y \\ \left(\mu + \frac{\mu_t}{\sigma_k}\right)\frac{\partial k}{\partial y} \\ \left(\mu + \frac{\mu_t}{\sigma_\varepsilon}\right)\frac{\partial \varepsilon_s}{\partial y} \end{pmatrix},$$

and the viscous stress tensor are expressed as

$$\sigma_{ij} = (\mu + \mu_t)\left(2\,\widetilde{S}_{ij} - \frac{2}{3}\frac{\partial\,\widetilde{u}_k}{\partial x_k}\delta_{ij}\right) - \frac{2}{3}\,\overline{\rho}\,k\delta_{ij},$$

where δ_{ij} is the Kronecker delta, S_{ij} is the mean strain rate tensor, μ is the coefficients of molecular viscosity calculated by the Sutherland formula and μ_t is the coefficients of eddy viscosity, respectively. The heat flux is calculated from

$$q_i = -\left(\mu\frac{c_p}{Pr} + \mu_t\frac{c_p}{Pr_t}\right)\frac{\partial\,\widetilde{T}}{\partial x_i},$$

so that the linear gradient hypothesis is used for the turbulent heat flux. c_p is the specific heat at constant pressure, Pr and Pr_t are the laminar and turbulent Prandtl numbers, respectively, and T is the temperature. A constant turbulent Prandtl number is used.

The eddy viscosity μ_t is calculated as

$$\mu_t = c_\mu\,\overline{\rho}\,k^2/\varepsilon_s.$$

The source terms $\mathbf{H}$ can be written as

$$\mathbf{H} = \left(0, 0, \alpha\,\overline{p}\,/r, 0, P_k - \overline{\rho}\,\varepsilon, c_{\varepsilon 1}P_k\frac{\varepsilon_s}{k} - c_{\varepsilon 2}\,\overline{\rho}\,\frac{\varepsilon\varepsilon_s}{k}\right)^T,$$

where P_k is the TKE production, ε is the total dissipation rate of TKE. In the cartesian coordinate system r and α are 1 and 0, respectively, and in the cylindrical coordinate system r and α are y and 1, respectively.

The total dissipation rate is decomposed into the solenoidal dissipation and the dilatation dissipation

$$\varepsilon = \varepsilon_s + \varepsilon_d.$$

In the "standard" $k - \varepsilon$ model [1] constants are

$$c_\mu = 0.09, \quad c_{\varepsilon 1} = 1.44, \quad c_{\varepsilon 2} = 1.92, \quad \sigma_k = 1, \quad \sigma_\varepsilon = 1.3.$$

3 Turbulence modeling

Compressibility and non-equilibrium of turbulence are two important phenomena for turbulence modeling in turbulent flow in rocket engine nozzles. Supersonic flow with large density gradients is realized in diffuser part of nozzle under flight conditions especially when shock waves are generated inside the nozzle. Such situation is typical for separated flow in nozzles.

As follows from DNS data the most important compressibility effect is the dilatation dissipation ε_d. We compared results of numerical simulation of several separated flows in plane and conical nozzles obtained with most dilatation dissipation models described in literature. Overall best results were obtained with models [2] and [3]

$$\varepsilon_d = \left(\alpha_1 \tilde{M}_t^2 + \alpha_2 \tilde{M}_t^4\right) \varepsilon_s, \tag{1}$$

where $\tilde{M}_t = \max(0, M_t - M_{t0})$. Values of constants are $\alpha_1 = 1$, $\alpha_2 = 0$, $M_{t0} = 0$ for the model [2] and $\alpha_1 = 1$, $\alpha_2 = 60$, $M_{t0} = 0.1$ for the model [3].

Due to gas dynamics discontinuities in flow field essentially non-equilibrium regions occurs near discontinuities where the production of TKE is considerable larger than the dissipation. Some non-equilibrium modifications of $k - \varepsilon$ model were studied on basis of numerical simulation of turbulent flows with discontinuities. Special attention was given to compatibility of non-equilibrium modifications with the dilatation dissipation models. We shall describe some studied non-equilibrium modifications of $k - \varepsilon$ model which will be used further.

The renormalization group (RNG) $k - \varepsilon$ model [4] can be considered as the non-equilibrium modification of $k - \varepsilon$ model

$$c_{\varepsilon 1} = 1.42\left(1 - \eta\left(1 - \eta/\eta_0\right)\left(1 + \beta\eta^3\right)\right), \tag{2}$$

where

$$\eta = \sqrt{\lambda / c_\mu}, \quad \eta_0 = 4.38, \quad \beta = 0.012.$$

The ratio of the production of TKE to the dissipation is denoted as $\lambda = P_k / (\overline{\rho}\,\varepsilon)$. The ratio can be considered as the non-equilibrium parameter. Other coefficients of the model are

$$c_{\varepsilon 2} = 1.68, \quad \sigma_k = 0.7179, \quad \sigma_\varepsilon = 0.7179, \quad c_\mu = 0.084.$$

The second non-equilibrium modification is the model [5] which is close to "extended" $k - \varepsilon$ model [6] and is more robust than [6]

$$c_{\varepsilon 1} = 1.44 + 0.3\left(\lambda' - 1\right) / \left(\lambda' + 1\right). \tag{3}$$

The modified non-equilibrium parameter λ' is used in the model which depends on "shear" part of the TKE production

$$P_k' = \mu_t \left(\left(\frac{\partial \widetilde{u}}{\partial y}\right)^2 + \left(\frac{\partial \widetilde{v}}{\partial x}\right)^2 \right).$$

The third modification was proposed in [7] to improve prediction of decaying turbulence at low Reynolds numbers

$$c_{\varepsilon 1} = 1.5, \quad c_{\varepsilon 2} = 1.9\left(1 - 0.11\exp\left(-R_t^2/36\right)\right). \tag{4}$$

4 Numerical method

To solve Navier-Stokes and $k-\varepsilon$ model equations we use a second order of accuracy in time and space Godunov-type method (see [8]). The second order of accuracy is obtained with the application of the MUSCL (monotonic upstream-centered scheme for conservation laws)-Runge-Kutta scheme with essentially two-dimensional reconstruction.

For near wall region the non-equilibrium wall function approach is used. TKE production limiter is used to provide proper dependence of the turbulent energy production term on the mean strain in regions of high velocity gradient.

5 Results and discussion

At first we validated our numerical code by means of comparison of our computed results of separated nozzle flows with experimental results by different authors. The first nozzle is an 11.01° half angle plane convergent–divergent nozzle [9] with a throat width of 27.5 *mm* and an exit width of 42.2 *mm* corresponding to an expansion ratio of 1.797, for a total length of 115.6 *mm*. The inlet temperature is 293°K, the ambient pressure is $p_a = 102387.14$ *Pa*, the ambient temperature is 293°K. The nozzle pressure ratio $n = p_0/p_a$ was varied in the experiment from 1.8 to 8.95.

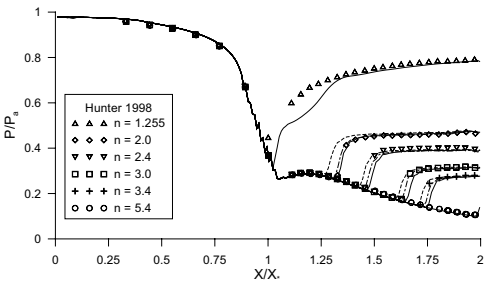

Fig. 1. Wall pressure data for plane nozzle [9]

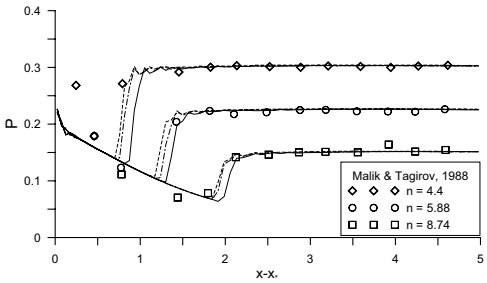

Fig. 2. Wall pressure data for conical nozzle [10]

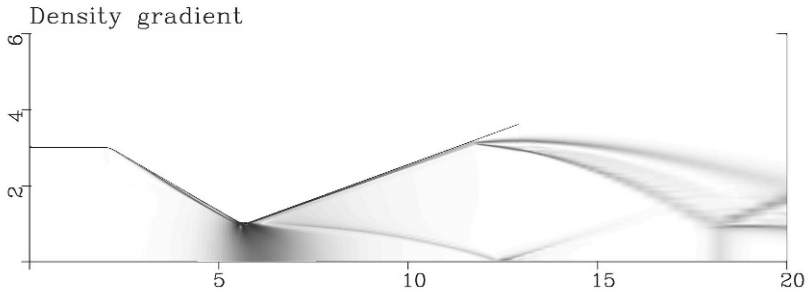

Fig. 3. Numerical Schlieren images of the flow field in the conical nozzle

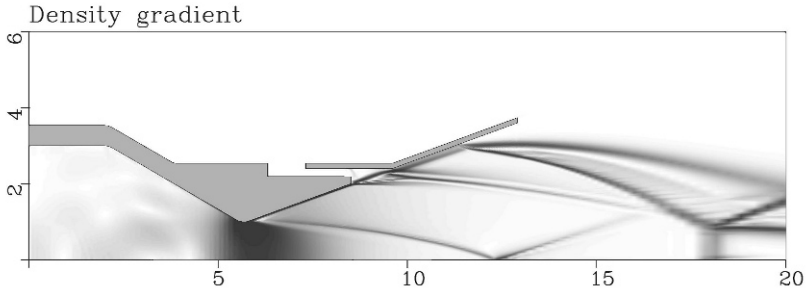

Fig. 4. Numerical Schlieren images of the flow field in the conical nozzle with one slot

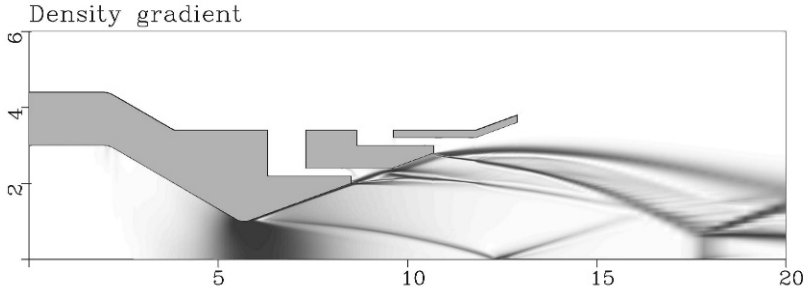

Fig. 5. Numerical Schlieren images of the flow field in the conical nozzle with two slots

Fig. 1 shows computed and measured [9] wall pressure distributions for different nozzle pressure ratios n. The solid, dashed and dash–doted lines correspond to the non-equilibrium modifications (3), (4) and (2), respectively. The dilatation model (1) is used. It can be seen that all three models allow to obtain a separation point position and a recovery pressure level in a recirculation zone after separation point with reasonable accuracy. We might observe in passing that the solution for $n = 1.255$ is unsteady regardless of used model and the shown curve corresponds to arbitrary time.

It is well known that $k - \varepsilon$ model predicts plane flows considerably better than axisymmetric. Therefore the second nozzle used for the validation is an 22.5° half angle conical convergent–divergent nozzle [10] with a throat radius of 5 *mm* and an exit radius of 16 *mm* corresponding to an expansion ratio of 10.24, for a conical part length of 26.52 *mm*. The inlet temperature is 293°K, the inlet pressure is $p_0 = 36$ *atm*, the ambient

temperature is 293°K. Three nozzle pressure ratios n were used in the experiment: 4.4, 5.88 and 8.74.

Fig. 2 shows computed and measured [10] wall pressure distributions for different nozzle pressure ratios n. The solid, dashed and dash–doted lines correspond to the non-equilibrium modifications (3), (4) and (2), respectively. The dilatation model (1) is used. As in the plane case accuracy of separation point and pressure recovery prediction is reasonable. Some discrepancy between measured and computed pressure before separation point can be explained by insufficient nozzle description in [10].

Results of numerical simulation of turbulent nozzle flow are shown on Fig. 3 for a smooth conical nozzle, on Fig. 4 for the same nozzle with one slot, and on Fig. 5 for the same nozzle with two slots. An half-angle of the conical nozzle supersonic part is 20°, a throat diameter is 10 *mm*, a slot width is 1 *mm*. The inlet temperature is 293°K, the ambient pressure is 101250 *Pa*, the ambient temperature is 293°K. The nozzle pressure ratio n is 40. The overexpanded flow regime with separation is realized under such conditions in the smooth nozzle (see Fig. 3). In the nozzle with single slot the separation occurs earlier (for smaller x) than in the smooth nozzle Fig. 4. The overexpanded flow zone decreases providing an increase in static thrust efficiency. In the nozzle with two slots the earliest separation occurs 5 and the overexpanded flow zone is smallest. Further numerical simulation shows that under high–altitude conditions the impulse loss due to a working fluid leakage through the circular slot is small and does not have a pronounced effect on thrust efficiency.

Acknowledgement. The presented research work was supported by the International Science Technical Center (ISTC) within the frames of the ISTC Project 2598.

References

1. Launder B.E., Spalding D.B. : Computer Meth. Appl. Mech. Engn., **3**, 3, 269–289, (1974)
2. Sarkar S., Erlebacher G., Hussaini M.Y., Kreiss H.O. : J. Fluid Mech., **227**, 473–493 (1991)
3. Dash S.M., Kenzakowski D.C., Seiner J.M., Bhat T.R.S. : AIAA Pap., 93–4390, (1993)
4. Yakhot V., Orszag S.A., Thangam S., Gatski T.B., Speziale C.G. : Phys. Fluids A, **4**, 7, 1510–1520, (1992)
5. Chen Y.S. : AIAA Pap., 86–0438, (1986)
6. Chen Y.S., Kim S.W. : NASA Contractor Report, 179204, (1987)
7. Hanjalic K., Launder B.E. : J. Fluid Mech., **52**, 609–638, (1972)
8. Ivanov I.E., Kryukov I.A. : Matematicheskoe modelirovanie RAN, **8**, 6, 47–55, (1996)
9. Hunter C.A. : AIAA Pap., 98-3107, (1998)
10. Malik T.I., Tagirov R.K. : Akademiia Nauk SSSR, Izvestiia, Mekhanika Zhidkosti i Gaza, 6, 60–66, (1988)